Defective extracellular pyrophosphate metabolism promotes vascular calcification in a mouse model of Hutchinson-Gilford progeria syndrome that is ameliorated upon pyrophosphate treatment

Ricardo Villa-Bellosta, Ph.D. [1], José Rivera-Torres, Ph.D.[1], Fernando G. Osorio, Msc[2], Rebeca Acín-Pérez, Ph.D.[3], José A. Enriquez, Ph.D.[3], Carlos López-Otín, Ph.D.[2], Vicente Andrés, Ph.D. [1,#]

[1] Department of Epidemiology, Atherothrombosis and Imaging, Centro Nacional de Investigaciones Cardiovasculares, Madrid, Spain.

[2] Departamento de Bioquímica y Biología Molecular. Universidad de Oviedo-IUOPA, Oviedo, Spain.

[3] Department of Cardiovascular Development and Repair, Centro Nacional de Investigaciones Cardiovasculares, Madrid, Spain.

 # Corresponding author: Centro Nacional de Investigaciones Cardiovasculares, Melchor Fernández Almagro 3, 28029 Madrid, Spain.

Telephone number: +34914531200, extension 1502

FAX number: +34914531245

Email: vandres@cnic.es

Total word count: 6782

Subject Codes: [130] Animal models of human disease; [97] Other Vascular biology

Running title: Defective extracellular pyrophosphate in HGPS

ABSTRACT

Background: Progerin is a mutant form of lamin A responsible for Hutchinson-Gilford progeria syndrome (HGPS), a premature aging disorder characterized by excessive atherosclerosis and vascular calcification that leads to premature death, predominantly from myocardial infarction or stroke. The goal of this study was to investigate mechanisms causing excessive vascular calcification in HGPS.

Methods and Results: We performed expression and functional studies in wild-type mice and knock-in *Lmna*$^{G609G/+}$ mice expressing progerin, which mimic the main clinical manifestations of HGPS. *Lmna*$^{G609G/+}$ mice showed excessive aortic calcification, and primary aortic vascular smooth muscle cells (VSMCs) from these progeroid animals have an impaired capacity to inhibit vascular calcification. This defect in progerin-expressing VSMCs is associated with increased tissue expression and activity of tissue-nonspecific alkaline phosphatase (TNAP) and mitochondrial dysfunction leading to reduced ATP synthesis. Accordingly, *Lmna*$^{G609G/+}$ VSMCs are defective for the production and extracellular accumulation of pyrophosphate, a major inhibitor of vascular calcification. We also found increased alkaline phosphatase activity and reduced ATP and pyrophosphate levels in plasma of *Lmna*$^{G609G/+}$ mice without changes in phosphorus and calcium. Treatment with pyrophosphate inhibited vascular calcification in progeroid mice.

Conclusions: Excessive vascular calcification in *Lmna*^{G609G} mice is caused by reduced extracellular accumulation of pyrophosphate resulting from increased TNAP activity and diminished ATP availability caused by mitochondrial dysfunction in VSMCs. Excessive calcification is ameliorated upon pyrophosphate treatment. These findings reveal a previously undefined pathogenic process in HGPS that may also contribute to vascular calcification in normal aging, since progerin progressively accumulates in the vascular tissue of non-HGPS individuals.

Key words: HGPS; progerin; vascular calcification; pyrophosphate; muscle, smooth.

Introduction

Hutchinson-Gilford progeria syndrome (HGPS) is an extremely rare sporadic genetic disorder that is characterized by accelerated cardiovascular disease and premature aging.[1, 2] Most (>90%) HGPS patients carry a non-inherited autosomal dominant de novo heterozygous mutation at codon 608 of the *LMNA* gene (c.1824C>T: GGC>GGT; p.G608G). This mutation activates a cryptic splice donor site, causing the synthesis of progerin. [1, 2] Expression of this lamin A mutant disrupts the nuclear membrane architecture and causes multiple cellular alterations, including impaired DNA repair capacity and abnormal higher-order chromatin organization, gene transcription and signal transduction.[3, 4] HGPS patients exhibit accelerated atherosclerosis and die at a mean age of 13.4 years (range, 8-21 years) predominantly from myocardial infarction or stroke.[5-7] Additional clinical HGPS manifestations include dermal and bone abnormalities, alopecia and joint contractures.[5, 8-16] Moreover, the aortas and aortic valves of HGPS patients are excessively calcified,[10-12] and arteries from old transgenic mice carrying a human bacterial artificial chromosome that harbors the common HGPS mutation accumulate calcium deposits that are absent in age-matched controls.[17] However, the mechanisms underlying excessive vascular calcification in HGPS remain unexplored.

Vascular calcification typically manifests as calcium-phosphate deposition (CPD) in distinct layers of the aortic wall.[18, 19] Calcium-phosphate deposits are composed of several members of the calcium orthophosphate family, including hydroxyapatite, octocalcium phosphate and amorphous calcium phosphate.[20] Medial calcification occurs within the elastin region of arteries and is almost exclusively associated with vascular smooth muscle cells (VSMCs). Elevated serum phosphorus (in the form of inorganic phosphate) is a major risk factor for vascular calcification.[21, 22] *In vitro* and *in vivo* studies have shown that elevated inorganic phosphate concentration in VSMCs triggers a transition to a bone-forming phenotype.[18, 19] This transition results in over-expression of osteochondrogenic markers, such as the transcription factor Runx2 (also named Cbfa1), which induces the expression of major bone matrix components.[18, 19]

Extracellular pyrophosphate (ePPi) directly blocks CPD *in vitro* and *in vivo* and is therefore a major endogenous inhibitor of vascular calcification.[23-26] Degradation of ePPi is catalyzed by tissue-nonspecific alkaline phosphatase (TNAP), which hydrolyzes PPi to inorganic phosphate. Importantly, calcification in *ex vivo* cultured rat aorta is induced by alkaline phosphatase and is prevented by TNAP inhibitors.[26, 27] TNAP is moreover up-regulated in the aortas of uremic rats, resulting in increased hydrolysis of ePPi and vascular calcification.[28] The main enzyme involved in ePPi synthesis, both in aorta and in cultured VSMCs, is the ectoenzyme nucleotide pyrophosphatase/phosphodiesterase-1 (eNPP1).[26, 29] Lack of eNPP1 leads to extensive and fatal arterial calcification in children and mice.[30, 31] The substrate for eNPP1 is ATP, which accumulates in the extracellular matrix via the action of several transporters,[32] such as the multiple-pass transmembrane protein ANK.[33]

To define the molecular mechanisms that lead to vascular calcification in HGPS, we analyzed *Lmna*^{G609G} knock-in mice, which express progerin as a consequence of aberrant splicing resulting from the *LMNA* c.1827C>T (p.G609G) mutation, equivalent to the human mutation c.1824C>T (p.G608G).[34] This new mouse model of progeria mimics the main clinical manifestations of human HGPS, including cardiovascular aberrations and premature death.[34] Our studies reveal profound alterations in ePPi homeostasis caused by progerin expression that exacerbate vascular calcification, which is inhibited by pyrophosphate treatment.

METHODS

Mice. Male *Lmna*$^{G609G/+}$, *Lmna*$^{G609G/G609G}$ and wild-type littermates were used.[34] Animal studies were approved by the local ethics committee and conformed to Directive 2010/63EU and Recommendation 2007/526/EC regarding the protection of animals used for experimental and other scientific purposes, enforced in Spanish law under Real Decreto 1201/2005.

Cell culture. VSMCs were prepared from thoracic aortas of 30-32-week-old mice as described previously.[35] Cells were grown in minimal essential medium (MEM) containing 1 mM L-glutamine, 100 IU/ml penicillin, 100 µg/ml streptomycin and 10% fetal bovine serum (FBS) at 37ºC in a humidified atmosphere at 5% CO_2. VSMCs were used at passages 5-10. Cells were grown to confluence and used after an overnight quiescence step (0.1% FBS). Calcification assays were performed on cells incubated for 7 days in MEM supplemented with 0.1% FBS and 2 mmol/L Pi as described previously.[35, 36] For phosphatase activity studies and ATP and PPi measurements, VSMCs were incubated in medium without Phenol Red.

Quantification of calcium deposition. Aortic arch and thoracic aorta from wild-type and *Lmna*$^{G609G/+}$ mice (n=5 per genotype) were included in OCT (Sakura, Netherlands), and 4-µm cross-sections were cut with a cryostat (Leica CM1950, Barcelona, Spain). Calcification in aortic tissue was revealed by Alizarin red staining as described.[35, 36] To quantify calcium deposits, 2-4 aortic cross-sections of each mouse were analyzed with ImageJ (http://imagej.nih.gov/ij/docs/guide).

To quantify calcium content in VSMCs, cells were treated with 0.6 HCl overnight at 4ºC and analyzed with a colorimetric QuantiChrom calcium assay kit (BioAssay Systems, Hayward, California).

Pyrophosphate treatment in vivo. PPi (Sigma, S6422) was dissolved in sterile saline (B.Braun Medical SA, Barcelona, Spain). 10-week-old *Lmna*$^{G609G/G609G}$ mice were treated with PPi for 9 weeks

(daily intraperitoneal injection, 100 mg/Kg/day) and the control group received saline (n=5 mice in each group). Quantification of aortic calcification was performed as indicated above.

Quantitative real-time PCR (qPCR). Total RNA was isolated from mouse aorta or VSMCs using Qiazol lysis reagent (Qiagen, Madrid, Spain). After DNase treatament, 2 µg RNA was reverse transcribed using the High capacity cDNA reverse transcription kit (Applied Biosystems, Madrid, Spain). qPCR was performed using Power SYBR Green in 384-well clear optical reaction plates on an ABI PRISM 7900HT Sequence Detection System following the manufacturer's instructions for calibrator normalization (Applied Biosystems). All reactions were carried out in triplicate. The primers used for amplification were as follows: 1) **BMP-2** (NM_007553): 5`-CACCGTGCGCAGCTTCCA-3` (forward), 5`-CCGGGCCGTTTTCCCACTCA-3` (reverse); 2) **Runx2** (NM_001146038.1): 5`-CAGATCCCAGGCAGGCACAGTC-3` (forward), 5`-ACAGCGGCGTGGTGGAGTG-3` (reverse); 3) **eNPP1** (NM_008813): 5`-GGATTGTGCCAATAAGGACT-3` (forward), 5`- CAAGAACTGTTGCTGCTGGAG -3` (reverse); 4) **TNAP** (NM_007431): 5`-CTATGTCTGGAACCGCACTGA-3` (forward), 5`-AGCCTTTGAGGTTTTTGGTCA -3` (reverse); 5) **Pit1** (NM_015747): 5`-CTGCTTCACGAGTGGGTAGAG-3` (forward), 5`- TGTAAACTACGGCACGGAAAC-3` (reverse); 6) **Pit2** (NM_011394): 5`-CTCTACAACGAGACCGTGGAA-3` (forward), 5`-CATGAAGCCAGAAAGAAGTGG -3` (reverse); 7) **ANK** (NM_020332): 5`-CATCCCCATCCTGTCTCTGTA-3` (forward), 5`- ACACGAAGAGGTTGACAATGG -3` (reverse); 8) **eNTPD1** (NM_009848): 5`-AGCCTCCACACAGATCACCTT-3` (forward), 5`-GCCACCACTTGAAACCTGAAT -3` (reverse); 9) **Fetuin A** (NM_013465): 5`-ATCGACAAAGTCAAGGTGTGG-3` (forward), 5`- CAACTTACGAACGTCCTCTGC -3` (reverse); 10) Matrix Gla-protein (NM_008597): 5`-AGGAGAAATGCCAACACCTTT-3` (forward), 5`- ACGAAACTCCACAACCAAATG -3` (reverse). Expression was quantified by the comparative C_T method, with correction for the expression of the endogenous control gene acidic ribosomal phosphoprotein P0 (RPLP0, accession number NM_007475).

Immunoblots and inmunohistochemistry. VSMC lysates were prepared in lysis buffer (0.1% SDS, 25 mM Tris-HCl pH 7.4 and protease inhibitors) and 30-50 µg protein were separated by SDS-PAGE and blotted to PVDF membrane as previously described.[35] The following primary antibodies were used: rabbit monoclonal anti-eNTPD1 (1/5000, ab108248, Abcam, Cambridge, UK), rabbit polyclonal anti-TNAP (1µg/ml, ab65834, Abcam), rabbit polyclonal anti-GFP (1/2500, ab6556, Abcam) and mouse monoclonal anti-α-Tubulin (1/5000, sc-8035, Santa Cruz biotechnology, USA). After incubation with appropriate secondary antibodies, blots were revealed using the ECL system (Millipore, Billerica, MA, USA). Mouse aortas were immunohistochemically stained with a rabbit polyclonal antibody to Runx2 (1/500, ab102711, Abcam).

Phosphatase activity and ATP hydrolysis assays. Phosphatase activity in VSMCs or plasma was measured using the pNPP phosphatase assay kit and the Quantichrom alkaline phosphatase assay kit (BioAssay Systems), respectively. ATP hydrolysis assays in VSMCs cultures were performed as previously described.[26] Briefly, cells were seeded in 12-well plates and incubated for the indicated times with 1µM ATP and 1 µCi/mL [γ^{32}P]ATP radiotracer (Perkin Elmer, Madrid, Spain). ATP, inorganic phosphate and PPi in the culture medium were then separated by chromatography on PEI-cellulose plates and were developed with 650 mM KH_2PO_4 pH 3. After autoradiography, spots were excised and counted by liquid scintillation.

ATP and pyrophosphate quantification. ePPi was measured using an enzyme-linked bioluminescence assay in which PPi reacts with adenosine 5'-phosphosulfate (A5508, Sigma) in the presence of ATP-sulfurylase (A8957, Sigma) to generate ATP [29]. For each sample, the blank (reaction without ATP-sulfurylase) was subtracted to obtain the true PPi amount. ATP was measured by a coupled luciferin/luciferase reaction using an ATP determination kit (Invitrogen, Paisley, UK).

Generation of retroviral vectors and stable cell lines. Wild-type pre-lamin A and progerin cDNAs were PCR amplified using as template a previously published construct[37] or Addgene plasmid #17663, respectively. Amplicons were inserted into pECFP vector (Clontech). Cyan fluorescent

protein (CFP)-pre-lamin A and progerin-CFP were then subcloned into pMSCVpuro retroviral vector (Clontech, Moustain View, CA) after digestion with XhoI/EcoRI to respectively generate pMSCVpuro/CFP-pre-lamin A (which is post-translationaly modified to generate mature lamin A) and pMSCVpuro/Progerin-CFP. Correct cloning of both plasmids was verified by DNA sequencing. The precise primer sequences and cloning strategies are available upon request. To generate retroviral stocks, 5×10^6 HEK-293T cells were plated in 100 mm dishes. After 12 h, cells were transfected (Lipofectamine 2000; Invitrogen) with 10 μg pCL-Ecotropic vector and 10 μg of the desired plasmid (pMSCVpuro/CFP-pre-lamin A or pMSCVpuro/Progerin-CFP). Two days post-transfection, supernatants were harvested and filtered to obtain retroviral stocks. Primary VSMCs prepared from the aortas of 8-week-old C57BL/6J mice were incubated for 4 hr at 37°C with retroviral supernatant supplemented with 4 μg/mL polybrene. After 3 rounds of infection, cells were washed once with PBS and cultured in growth medium in the presence of 1 μg/mL puromycin until complete selection was achieved (passages 6-7). The subpopulations of cells expressing the CFP recombinant proteins were obtained using a fluorescence-activated cell sorter (FACSAria III cell sorter, BD Bioscience, San José, CA, EE.UU.).

Mitochondrial assays. Mitochondrial ATP synthesis in digitonin-permeabilized VSMCs ($2x10^6$ cells) was measured by kinetic luminescence assay. Cytochrome c oxidase (COX) and citrate synthase (CS) enzymatic activities were measured in cell lysates (30–50 μg protein) as described,[38] and expressed as international units (IU) per mg protein. COX activity was normalized to CS, a Krebs cycle enzyme used as an index of mitochondrial mass.

Statistical analysis. Results are expressed as mean±SEM. For the studies shown in Figure 1, 2, 3, 4 and 5A, results were analyzed using unpaired Student's t-test with Welch's correction for two samples with possibly unequal variance. The results in Figure 5B were analyzed using paired Student's t-test. In all cases, statistical significance was assigned at $p<0.05$.

RESULTS

Vascular smooth muscle calcification is increased in progeroid *Lmna*$^{G609G/+}$ mice. HGPS patients carry the *LMNA* mutation in heterozygosis and express both lamin A and progerin.[1, 2] We therefore performed studies with heterozygous *Lmna*$^{G609G/+}$ mice that also express lamin A and progerin and have a significantly shortened lifespan (average 34 weeks, compared with more than 2 years for wild-type controls) [34]. We used 30-32-week-old *Lmna*$^{G609G/+}$ mice. Gross examination of Alizarin Red-stained vessels revealed prominent medial calcification in aortic arch and thoracic aorta of *Lmna*$^{G609G/+}$ compared with wild-type mice, and computer-assisted planimetric analysis showed statistically significant differences between genotypes (Fig.1A). Consistent with these findings, qPCR revealed that calcified aortas from *Lmna*$^{G609G/+}$ mice have high mRNA levels of BMP-2 and Runx2, two osteogenic markers expressed during vascular calcification, but no changes were observed in the anti-calcification agents matrix Gla-protein (MGP) and fetuin A (Fig.1B,C). Immunohistochemical analysis confirmed the increase in Runx2 expression in *Lmna*$^{G609G/+}$ aortas compared with aortas from wild-type mice (Fig.1D).

We next studied primary cultures of VSMCs isolated from aortic tissue of wild-type and *Lmna*$^{G609G/+}$ mice. Previous *in vitro* studies showed that CPD is more prominent with lysed VSMCs than with live cells, suggesting that VSMCs synthesize CPD inhibitors.[25, 35, 36] We therefore compared the CPD-inhibitory capacity of wild-type and *Lmna*$^{G609G/+}$ VSMCs. Cells were incubated for 7 days in calcifying medium, and the difference in CPD between lysed and live cells (ΔCa^{2+}) was calculated. *Lmna*$^{G609G/+}$ VSMCs showed a significantly lower capacity to inhibit calcium deposition than equivalent numbers of control cells, after normalization for protein concentration (Fig 1E).

***Lmna*$^{G609G/+}$ VSMCs have an impaired capacity to synthesize extracellular pyrophosphate.** Since excessive calcification in *Lmna*$^{G609G/+}$ aorta was not associated with reduced expression of MGP and fetuin A (Fig.1B), we quantified in VSMC-conditioned culture medium the accumulation of ePPi, the major endogenous inhibitor of vascular calcification.[21, 23-26] After 2 days in culture, ePPi

levels were 3.8-fold lower in *Lmna*$^{G609G/+}$ VSMCs compared with wild-type controls (Fig.2A). RT-PCR analysis of enzymes and transporters involved in ePPi metabolism demonstrated significantly higher expression of TNAP, Apyrase1/eNTPD1 and the phosphate transporter Pit2 in *Lmna*$^{G609G/+}$ compared with wild-type VSMCs, whereas eNPP1, ANK and Pit1 were unaffected (Fig.2B). Western blot analysis confirmed the increase in the ectoenzymes TNAP and eNTPD1 in *Lmna*$^{G609G/+}$ VSMCs (Fig.2C). Moreover, phosphatase activity was 2-fold higher in *Lmna*$^{G609G/+}$ VSMCs (Fig.2D).

Given these findings, we next investigated the capacity of *Lmna*$^{G609G/+}$ VSMCs to synthesize PPi using ATP as substrate. Cells were incubated for different times with 1 μM ATP and [γ^{32}P]-ATP radiotracer, and radioactive ATP, PPi and inorganic phosphate (Pi) were quantified in the culture medium after separation by thin-layer chromatography (Fig.2E). Wild-type and *Lmna*$^{G609G/+}$ VSMCs showed indistinguishable rates of ATP hydrolysis, with approximately 98% of ATP being hydrolyzed after 80 minutes (Fig.2E). However, the amount of ePPi produced was only 28% in *Lmna*$^{G609G/+}$ VSMCs, compared with 47% in wild-type cells, and the amount of Pi produced was 68% in *Lmna*$^{G609G/+}$ VSMCs compared with 49% in wild-type cells (Fig.2E). Accordingly, the Pi:PPi ratio increased from ≈1:1 in wild-type VSMCs to ≈2.4:1 in *Lmna*$^{G609G/+}$ VSMCs.

VSMCs expressing progerin have impaired ATP synthesis and mitochondrial function.

Extracellular ATP hydrolysis is the major source of ePPi in aorta and in VSMCs.[26] We therefore analyzed intracellular ATP levels and extracellular ATP accumulation in wild-type and *Lmna*$^{G609G/+}$ VSMCs. *Lmna*$^{G609G/+}$ VSMCs showed significantly lower levels of extracellular ATP (Fig.3A) and intracellular ATP (Fig.3B). *Lmna*$^{G609G/+}$ VSMCs also exhibited lower mitochondrial ATP production (Fig.3C). This was associated with a significantly lower COX/CS ratio (Fig.3D), indicating impaired activity of COX, an essential component of the mitochondrial electron transport chain.

To assess whether the alterations observed in *Lmna*$^{G609G/+}$ VSMCs are a direct consequence of progerin expression, we performed retrovirus-mediated gain-of-function experiments. Western blot analysis demonstrated CFP-lamin A and progerin-CFP expression in primary mouse VSMCs infected

with retrovirus encoding these proteins (Fig.4A). In agreement with many previous studies in different cell types, infected VSMCs expressed CFP-lamin A predominantly in the perinuclear rim, whereas progerin-CFP was found in both the perinuclear rim and in nucleoplasmic aggregates (Fig.4B). Compared with VSMCs expressing CFP-lamin A, forced progerin expression in VSMCs led to increased TNAP and Apyrase1/eNTPD1 mRNA steady-state levels without affecting the expression of others enzymes and transporters involved in ePPi metabolism (Fig.4C). Western blot analysis confirmed the increase in TNAP and eNTPD1 in *Lmna*$^{G609G/+}$ VSMCs overexpressing progerin (Fig.4D). Consistent with the results in primary *Lmna*$^{G609G/+}$ VSMCs, we also found significant reductions in extracellular and intracellular ATP concentration, mitochondrial ATP synthesis, COX/CS ratio, and ePPi levels in progerin-CFP-overexpressing VSMCs compared with CFP-lamin A-expressing controls (Fig.4E).

Progeroid mice have affected plasma parameters involved in vascular calcification. Since hyperphosphatemia and hypercalcemia lead to CPD,[19] we quantified inorganic phosphate and calcium in plasma from wild-type and *Lmna*$^{G609G/+}$ mice (Fig.5A). These parameters were similar in both genotypes (phosphorus: 8.2±0.2 in wild-type versus 7.7±0.3 mg/dl in *Lmna*$^{G609G/+}$; calcium: 14.4±0.3 in wild-type versus 14.8±0.3 mg/dl in *Lmna*$^{G609G/+}$; $p>0.05$). However, the plasma of *Lmna*$^{G609G/+}$ mice exhibited higher alkaline phosphatase activity (29.5% higher) and lower concentrations of ATP (8-fold) and ePPi (9-fold) (Fig.5A).

Pyrophosphate treatment inhibits aortic calcification in progeroid mice. Recent studies showed that injection of exogenous PPi prevents uremic vascular calcification in rats and mice.[24, 39] We therefore investigated the effect of PPi injection on vascular calcification in progeroid mice. For these studies, we used homozygous *Lmna*$^{G609G/G609G}$ mice, which are more severely affected than heterozygous *Lmna*$^{G609G/+}$ mice, with an average lifespan of only 103 days.[34] Ten-week-old homozygous *Lmna*$^{G609G/G609G}$ males received daily intraperitoneal injections of saline (control group) or PPi over 9 weeks (100 mg·kg^{-1}·day^{-1}, n=5 mice in each group). We did not observe differences in

body weight and mortality during follow-up, but post-mortem analysis demonstrated a statistically-significant reduction in aortic calcification in PPi-treated mice compared with controls, as revealed by planimetric analysis of Alizarin Red-stained aortic cross-sections (Fig.5B).

DISCUSSION

The aim of the present study was to identify molecular mechanisms that contribute to excessive vascular calcification in HGPS, a rare premature aging disorder caused by abnormal expression of progerin.[1, 2] Available evidence indicates that vascular calcification involves both passive and active processes[18, 19, 25] **(Fig.6).** CPD in the aortic wall and in *in vitro* models is the main feature of vascular calcification. At physiological serum concentrations of calcium and phosphate, CPD is a passive process that does not require cellular activity.[20, 25, 36, 40] Active processes involved in vascular calcification include reduced capacity of VSMCs to synthesize and secrete calcification inhibitors, such as MGP, fetuin A and ePPi, and the transition of VSMCs to a bone-forming phenotype, a process that is enhanced via CDP-dependent overexpression of osteochondrogenic factors, including Runx2.[18, 19, 36, 41] Pi is essential for the synthesis of ATP, the main source of ePPi.[26] It has thus been proposed that defective ATP production by VSMCs may impair the synthesis of CPD inhibitors.[42] Previous studies revealed that old transgenic mice carrying the common HGPS mutation exhibit a vascular calcification not seen in age-matched controls.[17] However, the mechanisms by which progerin exhacerbates vascular calcification remain unknown. Here, we have shown that progerin expression in *Lmna*$^{G609G/+}$ mice causes excessive vascular calcification associated with VSMC abnormalities that lead to impaired mitochondrial function and ATP production and reduced PPi synthesis **(Fig.6),** without affecting expression of the anti-calcification agents MGP and fetuin A. The causal relationship between progerin-induced low plasma ePPi and vascular calcification is

reinforced by our observation that aortic calcification in progeroid mice is reduced by treatment with PPi. It is noteworthy that physiological aging of non-HGPS individuals is associated with mitochondrial dysfunction[43, 44] and with a progressive accumulation of progerin in several tissues,[45-48] including vascular tissue.[6] Thus our findings might be relevant to vascular calcification not only in HGPS patients but also in the elderly.

Because HGPS patients carry the *LMNA* mutation in heterozygosis,[1, 2] we studied heterozygous *Lmna*$^{G609G/+}$ mice that express both lamin A and progerin.[34] We found excessive aortic calcification in progeroid *Lmna*$^{G609G/+}$ mice, which was associated with increased aortic expression of Runx2 and Bmp-2, two osteochondrogenic markers expressed in VSMCs during calcification *in vivo* and *in vitro*[19] that are induced by CPD.[36, 41] Importantly, VSMCs from *Lmna*$^{G609G/+}$ mice also exhibited an impaired capacity to inhibit CPD *in vitro,* which might explain the excessive medial calcification and the consequent overexpression of osteogenic markers in the aorta of *Lmna*$^{G609G/+}$ mice. To investigate the molecular mechanisms through which progerin triggers vascular calcification, we focused on the enzymes and transporters involved in ePPi homeostasis, a complex process that involves a balance between synthesis and degradation. Our results provide evidence that excessive vascular calcification in *Lmna*$^{G609G/+}$ mice is the consequence of alterations in VSMCs, including impaired synthesis of PPi, which leads to reduced accumulation of ePPi **(Fig.6).** Additional factors contributing to progerin-dependent reduction in ePPi levels include the upregulation of the ectoenzymes TNAP (the main enzyme involved in ePPi hydrolysis) and apyrase1/eNTPD1 (an enzyme that hydrolyzes ATP to release Pi), and low synthesis of ATP (the major substrate for ePPi synthesis). Our studies suggest that impaired ATP synthesis in *Lmna*$^{G609G/+}$ VSMCs is due to mitochondrial dysfunction associated with reduced complex IV COX activity. Importantly, retrovirus-mediated overexpression of progerin in wild-type VSMCs recapitulates the alterations observed in VSMCs isolated from *Lmna*$^{G609G/+}$ mice, including increased expression of TNAP and apyrase1/eNTPD1, reduced extracellular and intracellular ATP, diminished mitochondrial COX-CS ratio and ATP synthesis, and lower ePPi accumulation. A-type lamins have been linked to the regulation of multiple cellular processes (e.g.,

higher-order chromatin organization, DNA repair and replication, signal transduction, gene transcription, and cell proliferation, differentiation and migration), many of which are altered on progerin expression.[3, 4] Therefore additional studies are required to refine our understanding of the molecular mechanisms through which progerin expression alters VSMC behavior to promote calcification.

Hyperphosphatemia causes vascular calcification, thus underscoring the importance of Pi homeostasis in CPD. However, in a study of 15 HGPS patients with a wide age range of 1.6-17.8 years, Merideth et al.[5] reported a plasma phosphate concentration of 5.5±0.2 mg/dl, which is within the normal range in humans (2.7-5.5 mg/dl). We also found that *Lmna*$^{G609G/+}$ mice have plasma phosphorus concentrations in the normal range, undistinguishable from their wild-type littermates (≈8 mg/dl; normal range in mice: 5.7-9.2 mg/dl). Likewise, plasma calcium levels were normal in progeroid mice. These results indicate that hyperphosphatemia and hypercalcemia do not contribute to excessive vascular calcification in *Lmna*$^{G609G/+}$ mice, thus emphasizing the importance of reduced synthesis of ePPi by VSMCs as a key mechanism triggering excessive vascular calcification in HGPS. Although plasma phosphate levels are normal in *Lmna*$^{G609G/+}$ mice, increased accumulation of Pi in the tunica media may contribute to CPD in these animals, because the present results in primary VSMCs from *Lmna*$^{G609G/+}$ mice show augmented Pi production from ATP hydrolysis accompanied by a high Pi:PPi ratio of ≈2.4:1, compared with ≈1:1 in wild-type cells (Fig. 2E). The defect in ePPi production by progerin-expressing VSMCs is unlikely to be counterbalanced systemically, because PPi concentration in plasma from *Lmna*$^{G609G/+}$ mice was also significantly reduced compared with wild-type controls, probably as a result of lower ATP concentration and higher alkaline phosphatase activity in plasma. Our observation that PPi treatment inhibits aortic calcification in progeroid mice underscores the role of defective ePPi homeostasis as a key factor underlying excessive vascular calcification in HGPS. We did not observe changes in body weight or mortality upon PPi treatment. However, it is important to note that these studies were performed in homozygous *Lmna*$^{G609G/G609G}$ mice that have an average life span of only 15 weeks,[34] and treatment was started at 10 weeks of age,

when the animals already exhibit severe symptoms.[34] HGPS patients carry the *LMNA* mutation in heterozygosis,[1, 2] and therefore future studies are warranted in very young heterozygous *Lmna*$^{G609G/+}$ mice (1-2-weeks-old) to ascertain whether chronic treatment with PPi starting early in life, when symptoms are absent or very mild, can not only inhibit vascular calcification but also improve the general health and lifespan of progeroid mice.

Since imbalances in the degradation and synthesis of ePPi have been shown to lead to pathologic calcification of articular cartilage,[49] the systemic defect in circulating PPi associated with progerin expression might promote not only excessive vascular calcification but also the appearance of joint contractures, a characteristic of both HGPS patients[5] and *Lmna*^{G609G} mice.[34] Treatment with PPi might thus ameliorate both vascular calcification and joint contractures. It is noteworthy that combined treatment with statins and bisphosphonates (nonhydrolyzable pyrophosphate analogues) significantly extends the average lifespan of progeroid *Zmpste24*$^{-/-}$ mice, another model of premature aging caused by abnormal accumulation of prelamin A.[50] Based on these findings, ongoing clinical trials are assessing the efficacy of statin plus bisphosphonate (pravastatin plus zoledronate) with or without farnesyl transferase inhibitor (http://www.progeriaresearch.org/clinical_trial.html). However, although treatment with bisphosphonates decreases aortic calcification, animal studies have identified adverse effects of these compounds in bone.[51, 52] Moreover, bisphosphonates have been shown to induce the rupture of atherosclerotic plaques in apolipoprotein E-null mice.[53] In contrast, recent studies have shown that exogenous PPi injected daily into uremic rats and mice reduces the calcium content in calcified aortas without producing adverse effects on bone.[24, 39] Moreover, TNAP and PHOSPHO1 inhibitors can inhibit vascular calcification.[27, 54] Future studies in HGPS mouse models are thus warranted to investigate whether treatment with PPi in combination with TNAP or PHOSPHO1 inhibitors and FTI and statins is more beneficial than current strategies.

CLINICAL PERSPECTIVE

Progerin, a mutant form of lamin A, is responsible for Hutchinson-Gilford progeria syndrome (HGPS), a rare premature aging disorder featuring excessive vascular calcification (VC). Calcium dysfunction is under-studied in HGPS. Here, we show that progerin-expressing heterozygous *Lmna*$^{G609G/+}$ mice, which mimic the main clinical manifestations of HGPS, develop excessive VC. Moreover, primary vascular smooth muscle cells (VSMCs) from *Lmna*$^{G609G/+}$ mice exhibit above normal tissue-nonspecific alkaline phosphatase (TNAP) and apyrase 1/eNTPD1, and below normal mitochondrial ATP synthesis and extracellular ATP accumulation. Accordingly, *Lmna*$^{G609G/+}$ VSMCs show defective production and extracellular accumulation of pyrophosphate, a major inhibitor of VC. We also found elevated alkaline phosphatase activity and low ATP and pyrophosphate levels in plasma of *Lmna*$^{G609G/+}$ mice. Administration of pyrophosphate to severely ill progeroid *Lmna*$^{G609G/G609G}$ mice carrying the *LMNA* mutation in homozygosis inhibited VC but did not increase body weight or improve mortality. Because HGPS patients carry the *LMNA* mutation in heterozygosis, future studies are warranted in heterozygous *Lmna*$^{G609G/+}$ mice to ascertain whether chronic treatment with pyrophosphate starting early in life can not only inhibit VC but also improve general health and lifespan. It will also be of interest to determine whether anti-calcification treatment with pyrophosphate and TNAP or PHOSPHO1 inhibitors, in combination with the farnesyl transferase inhibitors and statins currently under evaluation in HGPS clinical trials, is more beneficial than current strategies. Since progerin progressively accumulates in the vascular tissue of non-HGPS individuals, these studies should shed light on VC associated with both premature and physiological aging.

ACKNOWLEDGEMENTS

We thank Simon Bartlett for English editing, María J. Andrés-Manzano for help preparing the figures, and Inés Ortega, Virginia Zorita and the CNIC's Animal Facility for care of mice.

FUNDING SOURCES

Work in the author's laboratory is supported by grants from the Ministerio de Economía y Competitividad (MINECO) (SAF2010-16044), Instituto de Salud Carlos III (RD06/0014/0021 and RD12/0042/0028) and the Progeria Research Foundation. R.V.-B. holds a Juan de la Cierva postdoctoral contract from MINECO (JCI-2011-09663). CL-O is an Investigator of the Botín Foundation. The Instituto Universitario de Oncología is supported by Obra Social Cajastur and the CNIC by MINECO and Fundación Pro-CNIC.

DISCLOSURES

None

REFERENCES

1. De Sandre-Giovannoli A, Bernard R, Cau P, Navarro C, Amiel J, Boccaccio I, Lyonnet S, Stewart CL, Munnich A, Le Merrer M, Levy N. Lamin a truncation in hutchinson-gilford progeria. *Science*. 2003;300:2055
2. Eriksson M, Brown WT, Gordon LB, Glynn MW, Singer J, Scott L, Erdos MR, Robbins CM, Moses TY, Berglund P, Dutra A, Pak E, Durkin S, Csoka AB, Boehnke M, Glover TW, Collins FS. Recurrent de novo point mutations in lamin a cause hutchinson-gilford progeria syndrome. *Nature*. 2003;423:293-298
3. Schreiber KH, Kennedy BK. When lamins go bad: Nuclear structure and disease. *Cell*. 2013;152:1365-1375
4. Andrés V, González JM. Role of a-type lamins in signaling, transcription, and chromatin organization. *J Cell Biol*. 2009;187:945-957
5. Merideth MA, Gordon LB, Clauss S, Sachdev V, Smith AC, Perry MB, Brewer CC, Zalewski C, Kim HJ, Solomon B, Brooks BP, Gerber LH, Turner ML, Domingo DL, Hart TC, Graf J, Reynolds JC, Gropman A, Yanovski JA, Gerhard-Herman M, Collins FS, Nabel EG, Cannon RO, 3rd, Gahl WA, Introne WJ. Phenotype and course of hutchinson-gilford progeria syndrome. *N Engl J Med*. 2008;358:592-604
6. Olive M, Harten I, Mitchell R, Beers J, Djabali K, Cao K, Erdos MR, Blair C, Funke B, Smoot L, Gerhard-Herman M, Machan JT, Kutys R, Virmani R, Collins FS, Wight TN, Nabel EG, Gordon LB. Cardiovascular pathology in hutchinson-gilford progeria: Correlation with the vascular pathology of aging. *Arterioscler Thromb Vasc Biol*. 2010;30:2301-2309
7. Gerhard-Herman M, Smoot LB, Wake N, Kieran MW, Kleinman ME, Miller DT, Schwartzman A, Giobbie-Hurder A, Neuberg D, Gordon LB. Mechanisms of premature vascular aging in children with hutchinson-gilford progeria syndrome. *Hypertension*. 2012;59:92-97
8. Baker PB, Baba N, Boesel CP. Cardiovascular abnormalities in progeria. Case report and review of the literature. *Arch Pathol Lab Med*. 1981;105:384-386
9. Stehbens WE, Wakefield SJ, Gilbert-Barness E, Olson RE, Ackerman J. Histological and ultrastructural features of atherosclerosis in progeria. *Cardiovasc Pathol*. 1999;8:29-39
10. Nair K, Ramachandran P, Krishnamoorthy KM, Dora S, Achuthan TJ. Hutchinson-gilford progeria syndrome with severe calcific aortic valve stenosis and calcific mitral valve. *J Heart Valve Dis*. 2004;13:866-869
11. Salamat M, Dhar PK, Neagu DL, Lyon JB. Aortic calcification in a patient with hutchinson-gilford progeria syndrome. *Pediatr Cardiol*. 2010;31:925-926
12. Hanumanthappa NB, Madhusudan G, Mahimarangaiah J, Manjunath CN. Hutchinson-gilford progeria syndrome with severe calcific aortic valve stenosis. *Ann Pediatr Cardiol*. 2011;4:204-206
13. Kim HK, Lee JY, Bae EJ, Oh PS, Park WI, Lee DS, Kim JI, Lee HJ. Hutchinson-gilford progeria syndrome with g608g lmna mutation. *J Korean Med Sci*. 2011;26:1642-1645
14. Sowmiya R, Prabhavathy D, Jayakumar S. Progeria in siblings: A rare case report. *Indian J Dermatol*. 2011;56:581-582
15. Gordon CM, Gordon LB, Snyder BD, Nazarian A, Quinn N, Huh S, Giobbie-Hurder A, Neuberg D, Cleveland R, Kleinman M, Miller DT, Kieran MW. Hutchinson-gilford progeria is a skeletal dysplasia. *J Bone Miner Res*. 2011;26:1670-1679

16. Cleveland RH, Gordon LB, Kleinman ME, Miller DT, Gordon CM, Snyder BD, Nazarian A, Giobbie-Hurder A, Neuberg D, Kieran MW. A prospective study of radiographic manifestations in hutchinson-gilford progeria syndrome. *Pediatr Radiol*. 2012;42:1089-1098
17. Varga R, Eriksson M, Erdos MR, Olive M, Harten I, Kolodgie F, Capell BC, Cheng J, Faddah D, Perkins S, Avallone H, San H, Qu X, Ganesh S, Gordon LB, Virmani R, Wight TN, Nabel EG, Collins FS. Progressive vascular smooth muscle cell defects in a mouse model of hutchinson-gilford progeria syndrome. *Proceedings of the National Academy of Sciences of the United States of America*. 2006;103:3250-3255
18. Rutsch F, Nitschke Y, Terkeltaub R. Genetics in arterial calcification: Pieces of a puzzle and cogs in a wheel. *Circ Res*. 2011;109:578-592
19. Shanahan CM, Crouthamel MH, Kapustin A, Giachelli CM. Arterial calcification in chronic kidney disease: Key roles for calcium and phosphate. *Circ Res*. 2011;109:697-711
20. Johnsson MS, Nancollas GH. The role of brushite and octacalcium phosphate in apatite formation. *Crit Rev Oral Biol Med*. 1992;3:61-82
21. Alfrey AC, Ibels LS. Role of phosphate and pyrophosphate in soft tissue calcification. *Adv Exp Med Biol*. 1978;103:187-193
22. Block GA, Hulbert-Shearon TE, Levin NW, Port FK. Association of serum phosphorus and calcium x phosphate product with mortality risk in chronic hemodialysis patients: A national study. *Am J Kidney Dis*. 1998;31:607-617
23. Schibler D, Russell RG, Fleisch H. Inhibition by pyrophosphate and polyphosphate of aortic calcification induced by vitamin d3 in rats. *Clin Sci*. 1968;35:363-372
24. O'Neill WC, Lomashvili KA, Malluche HH, Faugere MC, Riser BL. Treatment with pyrophosphate inhibits uremic vascular calcification. *Kidney Int*. 2011;79:512-517
25. Villa-Bellosta R, Sorribas V. Calcium phosphate deposition with normal phosphate concentration. -role of pyrophosphate. *Circ J*. 2011;75:2705-2710
26. Villa-Bellosta R, Wang X, Millan JL, Dubyak GR, O'Neill WC. Extracellular pyrophosphate metabolism and calcification in vascular smooth muscle. *Am J Physiol Heart Circ Physiol*. 2011;301:H61-68
27. Narisawa S, Harmey D, Yadav MC, O'Neill WC, Hoylaerts MF, Millan JL. Novel inhibitors of alkaline phosphatase suppress vascular smooth muscle cell calcification. *J Bone Miner Res*. 2007;22:1700-1710
28. Lomashvili KA, Garg P, Narisawa S, Millan JL, O'Neill WC. Upregulation of alkaline phosphatase and pyrophosphate hydrolysis: Potential mechanism for uremic vascular calcification. *Kidney Int*. 2008;73:1024-1030
29. Prosdocimo DA, Douglas DC, Romani AM, O'Neill WC, Dubyak GR. Autocrine atp release coupled to extracellular pyrophosphate accumulation in vascular smooth muscle cells. *Am J Physiol Cell Physiol*. 2009;296:C828-839
30. Rutsch F, Ruf N, Vaingankar S, Toliat MR, Suk A, Hohne W, Schauer G, Lehmann M, Roscioli T, Schnabel D, Epplen JT, Knisely A, Superti-Furga A, McGill J, Filippone M, Sinaiko AR, Vallance H, Hinrichs B, Smith W, Ferre M, Terkeltaub R, Nurnberg P. Mutations in enpp1 are associated with 'idiopathic' infantile arterial calcification. *Nat Genet*. 2003;34:379-381
31. Johnson K, Polewski M, van Etten D, Terkeltaub R. Chondrogenesis mediated by ppi depletion promotes spontaneous aortic calcification in npp1-/- mice. *Arterioscler Thromb Vasc Biol*. 2005;25:686-691
32. Lohman AW, Billaud M, Isakson BE. Mechanisms of atp release and signaling in the blood vessel wall. *Cardiovasc Res*. 2012;95:269-280

33. Costello JC, Rosenthal AK, Kurup IV, Masuda I, Medhora M, Ryan LM. Parallel regulation of extracellular atp and inorganic pyrophosphate: Roles of growth factors, transduction modulators, and ank. *Connect Tissue Res*. 2011;52:139-146

34. Osorio FG, Navarro CL, Cadinanos J, Lopez-Mejia IC, Quiros PM, Bartoli C, Rivera J, Tazi J, Guzman G, Varela I, Depetris D, de Carlos F, Cobo J, Andres V, De Sandre-Giovannoli A, Freije JM, Levy N, Lopez-Otin C. Splicing-directed therapy in a new mouse model of human accelerated aging. *Sci Transl Med*. 2011;3:106ra107

35. Villa-Bellosta R, Sorribas V. Phosphonoformic acid prevents vascular smooth muscle cell calcification by inhibiting calcium-phosphate deposition. *Arterioscler Thromb Vasc Biol*. 2009;29:761-766

36. Villa-Bellosta R, Millan A, Sorribas V. Role of calcium-phosphate deposition in vascular smooth muscle cell calcification. *Am J Physiol Cell Physiol*. 2011;300:C210-220

37. Lattanzi G, Columbaro M, Mattioli E, Cenni V, Camozzi D, Wehnert M, Santi S, Riccio M, Del Coco R, Maraldi NM, Squarzoni S, Foisner R, Capanni C. Pre-lamin a processing is linked to heterochromatin organization. *Journal of cellular biochemistry*. 2007;102:1149-1159

38. Birch-Machin MA, Turnbull DM. Assaying mitochondrial respiratory complex activity in mitochondria isolated from human cells and tissues. *Methods Cell Biol*. 2001;65:97-117

39. Riser BL, Barreto FC, Rezg R, Valaitis PW, Cook CS, White JA, Gass JH, Maizel J, Louvet L, Drueke TB, Holmes CJ, Massy ZA. Daily peritoneal administration of sodium pyrophosphate in a dialysis solution prevents the development of vascular calcification in a mouse model of uraemia. *Nephrol Dial Transplant*. 2011;26:3349-3357

40. Schinke T, Karsenty G. Vascular calcification--a passive process in need of inhibitors. *Nephrol Dial Transplant*. 2000;15:1272-1274

41. Sage AP, Lu J, Tintut Y, Demer LL. Hyperphosphatemia-induced nanocrystals upregulate the expression of bone morphogenetic protein-2 and osteopontin genes in mouse smooth muscle cells in vitro. *Kidney Int*. 2011;79:414-422

42. Wang C, Li Y, Shi L, Ren J, Patti M, Wang T, de Oliveira JR, Sobrido MJ, Quintans B, Baquero M, Cui X, Zhang XY, Wang L, Xu H, Wang J, Yao J, Dai X, Liu J, Zhang L, Ma H, Gao Y, Ma X, Feng S, Liu M, Wang QK, Forster IC, Zhang X, Liu JY. Mutations in slc20a2 link familial idiopathic basal ganglia calcification with phosphate homeostasis. *Nat Genet*. 2012;44:254-256

43. Sahin E, Depinho RA. Axis of ageing: Telomeres, p53 and mitochondria. *Nat Rev Mol Cell Biol*. 2012;13:397-404

44. Green DR, Galluzzi L, Kroemer G. Mitochondria and the autophagy-inflammation-cell death axis in organismal aging. *Science*. 2011;333:1109-1112

45. Scaffidi P, Misteli T. Lamin a-dependent nuclear defects in human aging. *Science*. 2006;312:1059-1063

46. Cao K, Capell BC, Erdos MR, Djabali K, Collins FS. A lamin a protein isoform overexpressed in hutchinson-gilford progeria syndrome interferes with mitosis in progeria and normal cells. *Proc. Natl. Acad. Sci. USA.* 2007;104:4949-4954

47. McClintock D, Ratner D, Lokuge M, Owens DM, Gordon LB, Collins FS, Djabali K. The mutant form of lamin a that causes hutchinson-gilford progeria is a biomarker of cellular aging in human skin. *PLoS One*. 2007;2:e1269

48. Rodriguez S, Coppede F, Sagelius H, Eriksson M. Increased expression of the hutchinson-gilford progeria syndrome truncated lamin a transcript during cell aging. *Eur J Hum Genet*. 2009;17:928-937

49. Johnson K, Terkeltaub R. Inorganic pyrophosphate (ppi) in pathologic calcification of articular cartilage. *Front Biosci*. 2005;10:988-997

50. Varela I, Pereira S, Ugalde AP, Navarro CL, Suarez MF, Cau P, Cadinanos J, Osorio FG, Foray N, Cobo J, de Carlos F, Levy N, Freije JM, Lopez-Otin C. Combined treatment with statins and aminobisphosphonates extends longevity in a mouse model of human premature aging. *Nat Med*. 2008;14:767-772

51. Price PA, Faus SA, Williamson MK. Bisphosphonates alendronate and ibandronate inhibit artery calcification at doses comparable to those that inhibit bone resorption. *Arteriosclerosis, thrombosis, and vascular biology*. 2001;21:817-824

52. Lomashvili KA, Monier-Faugere MC, Wang X, Malluche HH, O'Neill WC. Effect of bisphosphonates on vascular calcification and bone metabolism in experimental renal failure. *Kidney Int*. 2009;75:617-625

53. Shimshi M, Abe E, Fisher EA, Zaidi M, Fallon JT. Bisphosphonates induce inflammation and rupture of atherosclerotic plaques in apolipoprotein-e null mice. *Biochem Biophys Res Commun*. 2005;328:790-793

54. Kiffer-Moreira T, Yadav MC, Zhu D, Narisawa S, Sheen C, Stec B, Cosford ND, Dahl R, Farquharson C, Hoylaerts MF, Macrae VE, Millan JL. Pharmacological inhibition of phospho1 suppresses vascular smooth muscle cell calcification. *J Bone Miner Res*. 2013;28:81-91

FIGURE LEGENDS

Figure 1. Excessive calcification in aorta and vascular smooth muscle cells from *Lmna*$^{G609G/+}$ mice. Thirty- to 32-week-old male *Lmna*$^{G609G/+}$ and wild-type mice and derived VSMCs were analyzed. (A) Representative images (x20) of Alizarin red staining and quantification of calcium deposition averaged from 2 to 4 aortic cross-sections for each mouse (n=5 mice per genotype). (B, C) qPCR analysis of the osteogenic markers BMP-2 and Runx2 and the calcification inhibitors matrix-Gla protein (MGP) and fetuin A in aorta. Results are means±SEM and are normalized to the level in wild-type mice (n=5 per genotype). (D) Representative images of aortic cross-sections immunostained for Runx2 in wild-type and *Lmna*$^{G609G/+}$ mice. The left panel shows the absence of staining in control experiments with secondary antibody but without anti-Runx2 antibody. (E) Live or lysed VSMCs were maintained in medium containing 1 mM Pi (non-calcifying media) or 2 mM Pi (pro-calcifying media) and calcium deposition was measured and normalized to protein content. The graph on the left shows the results of a representative experiment (means±SEM of six independent wells). The graph on the right shows the inhibition of calcium deposition in pro-calcifying media calculated as the difference between lysed and live cells for each genotype (means±SEM of three independent experiments performed with cells pooled from 10 mice per genotype). **: $p<0.01$, and $^{\#}$: $p<0.0001$ versus wild-type.

Figure 2. VSMCs expressing progerin exhibit impaired ATP-dependent PPi synthesis and extracellular PPi accumulation. Primary VSMCs were obtained from wild-type and *Lmna*$^{G609G/+}$ mice. (A) Quantification of ePPi accumulated over 2 days in culture. (B) qPCR analysis of ectoenzymes and transporters involved in vascular calcification. (C) Representative immunoblots and quantification of TNAP and eNTPD1 expression after normalization to α-tubulin (a.u., arbitrary units). (D) Alkaline phosphatase activity. Results in A-D are means±SEM of 3 independent experiments. (E) Cells were incubated with 1µM ATP plus 1 µCi/mL [γ^{32}P]ATP. At time points

indicated in the graphs, inorganic phosphate (Pi), PPi and ATP in the culture medium were separated by thin-layer chromatography. A representative autoradiograph is shown in the left. The graphs show the quantification of ATP, Pi and PPi. Results are means±SEM of six wells. Similar results were obtained in two additional experiments. *: $p<0.05$, **: $p<0.01$ and $^{\#}$: $p<0.0001$ versus wild-type.

Figure 3. VSMCs from progeroid *Lmna*$^{G609G/+}$ mice have low ATP levels and mitochondrial dysfunction. Wild-type and *Lmna*$^{G609G/+}$VSMCs were cultured to quantify the level of extracellular ATP (A), intracellular ATP (B), mitochondrial ATP synthesis (C), and the COX/CS activity ratio (D). Results are means±SEM of 12 determinations in two-three independent experiments. $^{\#}$: $p<0.0001$.

Figure 4. Forced progerin expression in VSMCs induces alterations in extracellular PPi metabolism. Primary VSMCs obtained from wild-type mice were infected with retroviral vectors encoding CFP-Lamin A or progerin-CFP. (A) Western blot analysis using anti-GFP antibody. (B) Confocal microscopy to visualize CFP-lamin A and progerin-CFP. (C) qPCR of enzymes and transporters involved in ePPi metabolism. Results are normalized to the mRNA levels in CFP-lamin A controls. (D) Representative immunoblots and quantification of TNAP and eNTPD1 expression after normalization to α-tubulin (a.u., arbitrary units). (E) Determination of extracellular and intracellular ATP, mitochondrial ATP synthesis, COX/CS ratio, and ePPi. Results are means±SEM of three independent experiments. *: $p<0.05$, **: $p<0.01$, ***: $p<0.001$ and $^{\#}$: $p<0.0001$ versus CFP-Lamin A.

Figure 5. PPi homeostasis in mouse plasma and treatment with exogenous PPi. (A) The indicated parameters were analyzed in plasma of 30-32-week-old male wild-type and *Lmna*$^{G609G/+}$ mice. Results are means±SEM of 8-10 mice. (B) Ten-week-old male *Lmna*$^{G609G/G609G}$ mice received for 9 weeks a daily ip injection of saline or exogenous PPi (n=5 mice in each group). Images show representative examples of Alizarin red-stained aortic tissue (boxed areas are shown at higher magnification). The graph shows quantification of calcium deposition by planimetric analysis of stained cross-sections. ***: $p<0.001$ and $^{\#}$: $p<0.0001$.

Figure 6. Proposed model of altered pyrophosphate homeostasis in HGPS. ePPi is a major inhibitor of calcium phosphate deposition that is synthesized from ATP by eNPP1 and degraded to Pi by TNAP. Pit1 and Pit2 mediate the cellular uptake of Pi, which is essential for ATP synthesis, mainly via mitochondrial oxidative phosphorylation. ATP is released to the extracellular matrix via the transporter ANK. Progerin expression in VSMCs augments TNAP and apyrase1/eNTPD1 and impairs mitochondrial function and ATP synthesis. These alterations lead to reduced extracellular concentrations of PPi and a high Pi:PPi ratio in the arterial wall. The plasma of *Lmna*$^{G609G/+}$ mice exhibits normal phosphorus and calcium levels, but higher alkaline phosphatase activity (ALP) and lower concentrations of ATP and ePPi. These alterations in VSMCs and blood of progeroid *Lmna*^{G609G} mice promotes excessive aortic calcification that can be inhibited upon treatment with PPi.

FIGURE 1

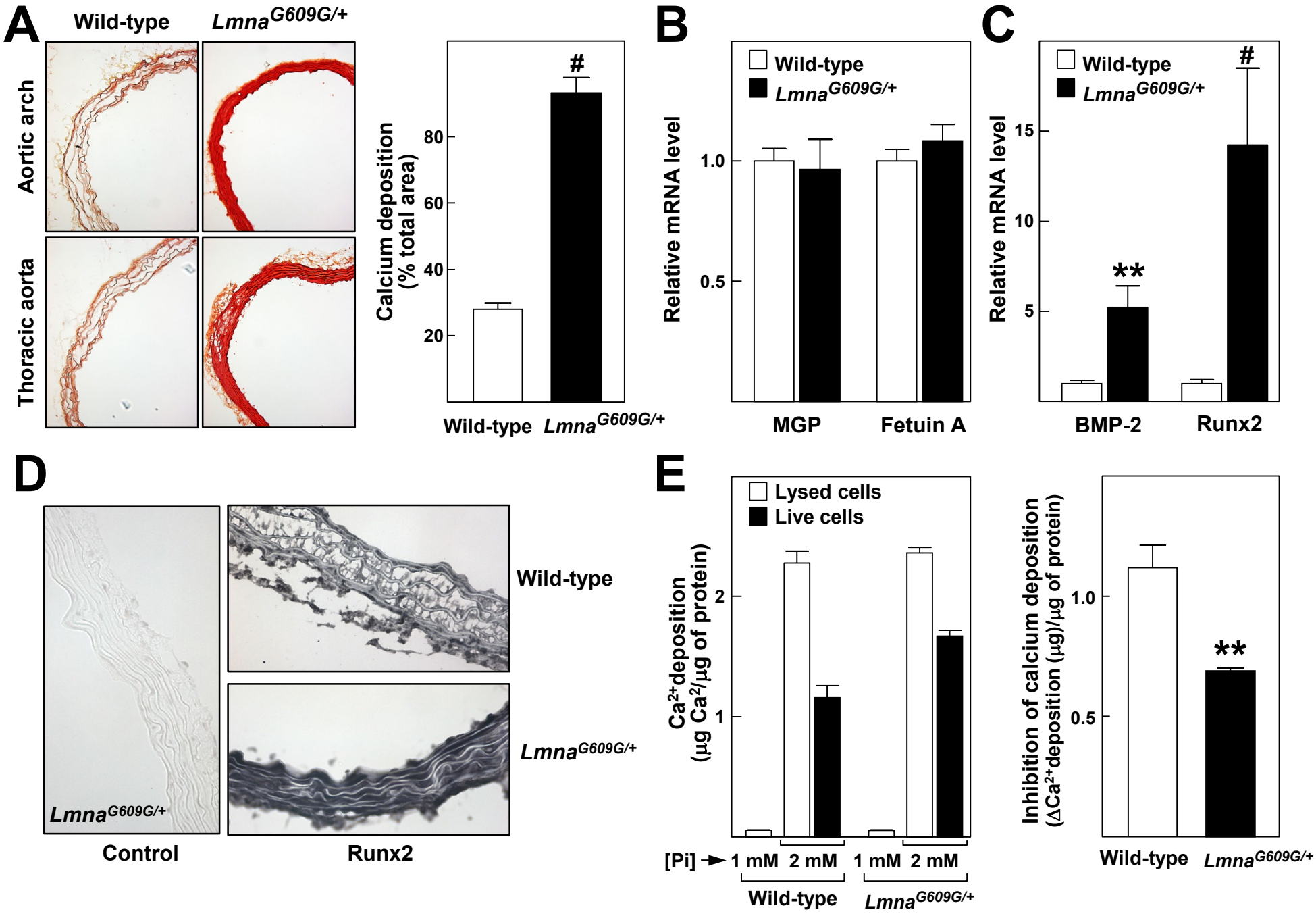
A
Wild-type
Lmna G609G/+
Aortic arch
Thoracic aorta
Calcium deposition (% total area)
#
Wild-type
Lmna G609G/+
B
Wild-type
Lmna G609G/+
Relative mRNA level
MGP
Fetuin A
C
Wild-type
Lmna G609G/+
Relative mRNA level
**
#
BMP-2
Runx2
D
Lmna G609G/+
Control
Runx2
Wild-type
Lmna G609G/+
E
Lysed cells
Live cells
Ca2+deposition (μg Ca2/μg of protein)
[Pi]
1 mM
2 mM
1 mM
2 mM
Wild-type
Lmna G609G/+
Inhibition of calcium deposition (ΔCa2+deposition (μg)/μg of protein)
**
Wild-type
Lmna G609G/+

FIGURE 2

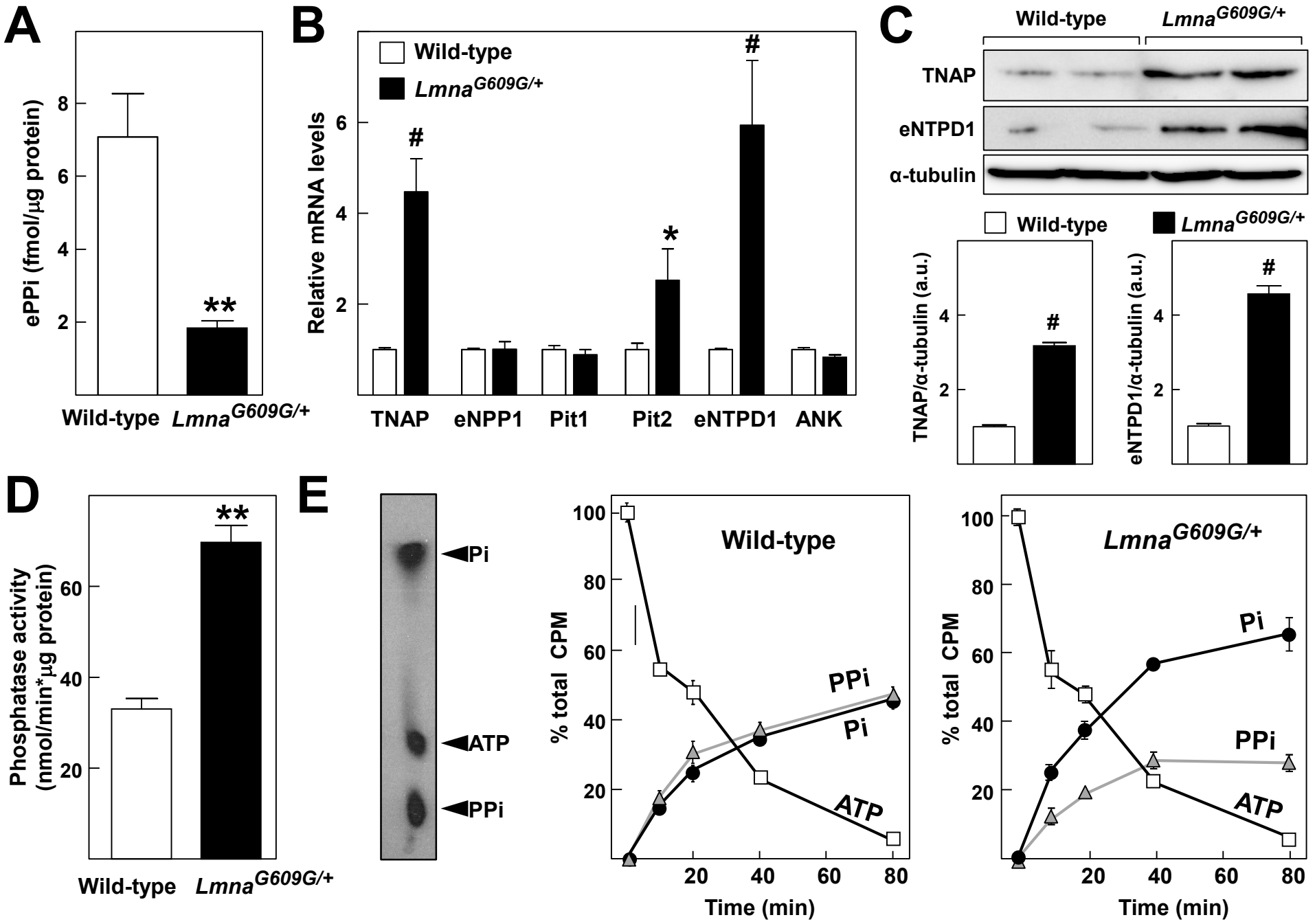
A
ePPi (fmol/µg protein)
Wild-type
Lmna G609G/+
B
Relative mRNA levels
Wild-type
Lmna G609G/+
TNAP
eNPP1
Pit1
Pit2
eNTPD1
ANK
C
Wild-type
Lmna G609G/+
TNAP
eNTPD1
α-tubulin
TNAP/α-tubulin (a.u.)
eNTPD1/α-tubulin (a.u.)
D
Phosphatase activity (nmol/min*µg protein)
E
Pi
ATP
PPi
% total CPM
Time (min)

FIGURE 3

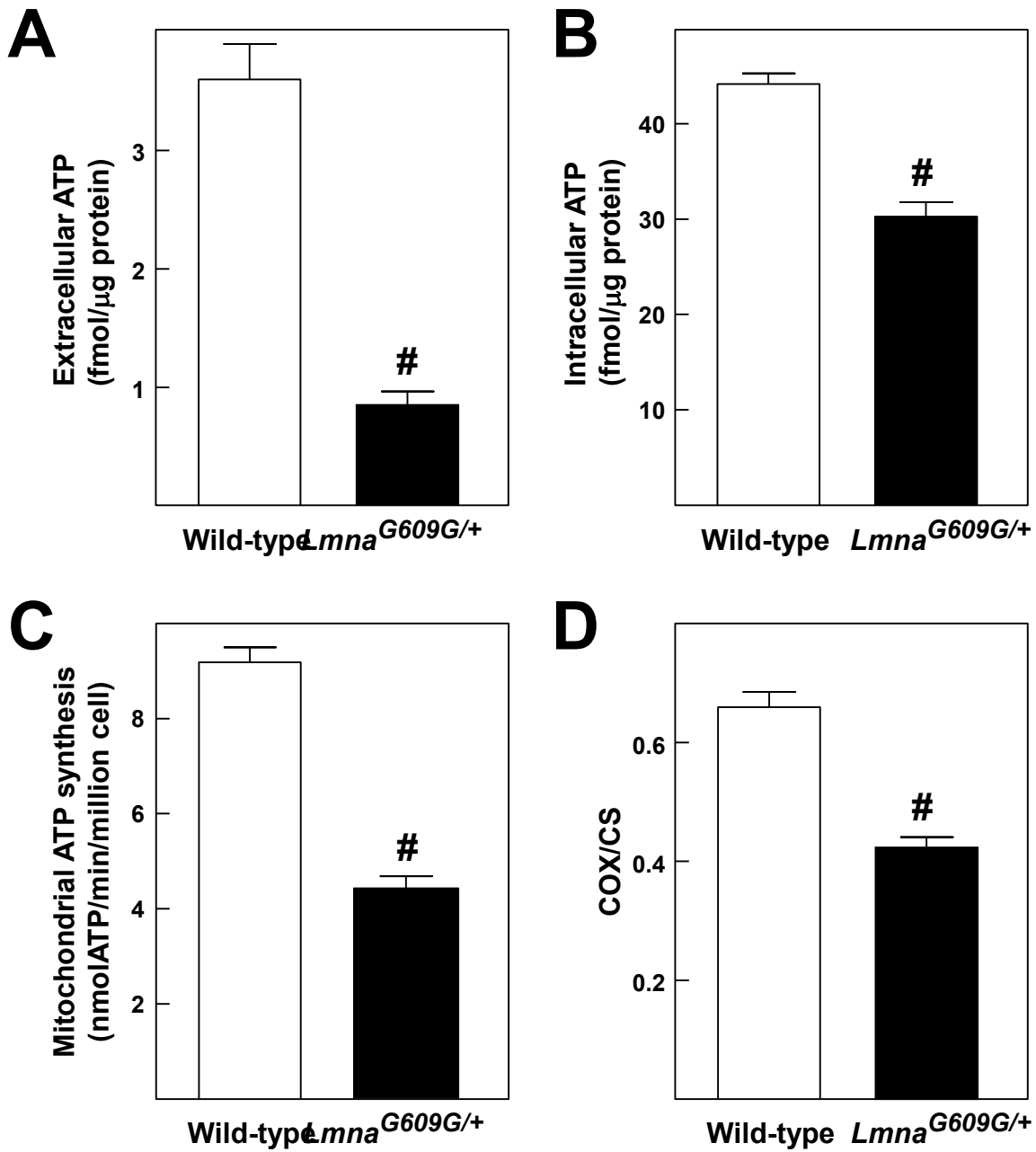
A
Extracellular ATP
(fmol/μg protein)
3
2
1
#
Wild-type
Lmna G609G/+
B
Intracellular ATP
(fmol/μg protein)
40
30
20
10
#
Wild-type
Lmna G609G/+
C
Mitochondrial ATP synthesis
(nmolATP/min/million cell)
8
6
4
2
#
Wild-type
Lmna G609G/+
D
COX/CS
0.6
0.4
0.2
#
Wild-type
Lmna G609G/+

FIGURE 4

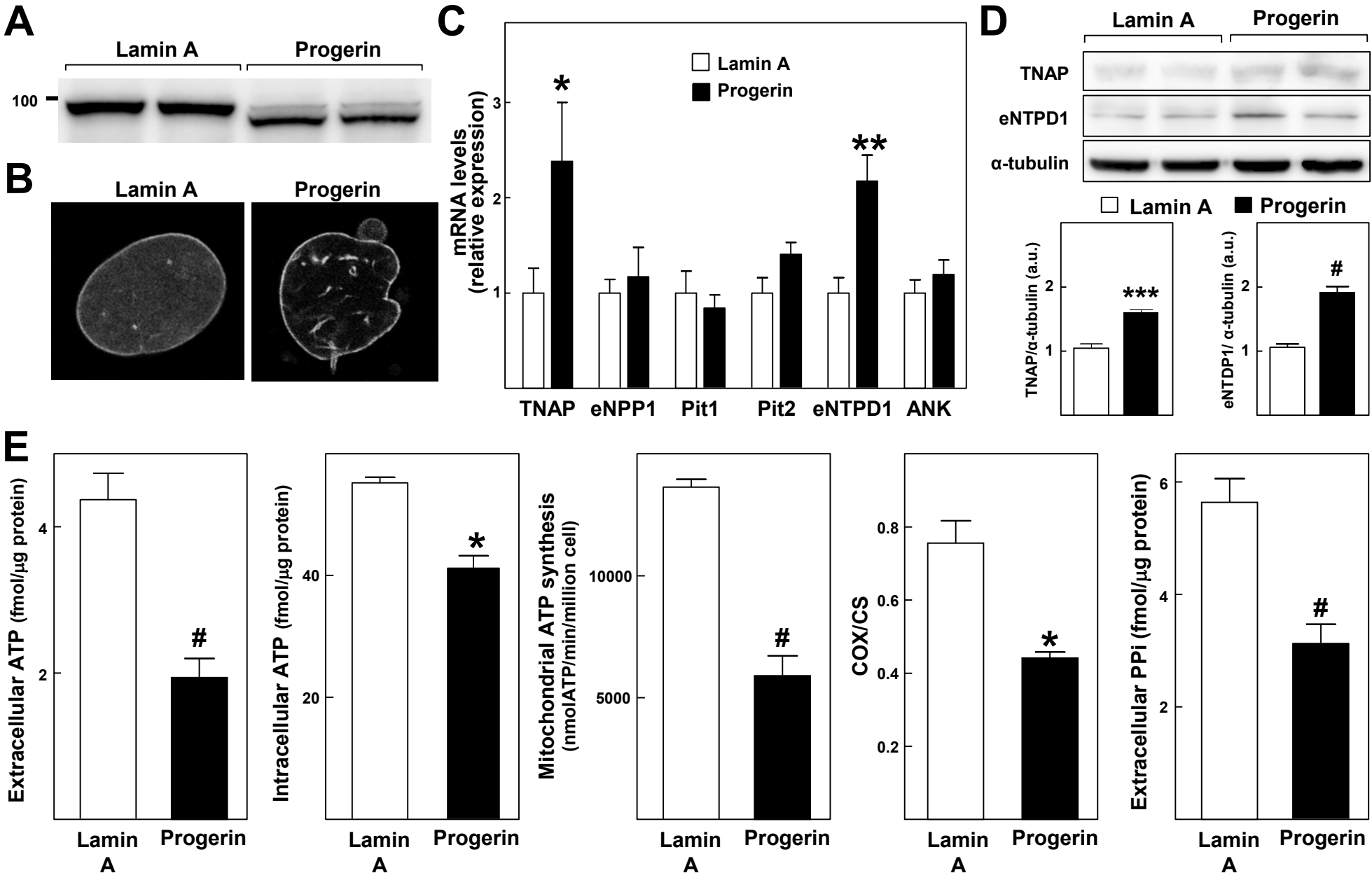
A
Lamin A
Progerin
100
B
Lamin A
Progerin
C
Lamin A
Progerin
mRNA levels (relative expression)
*
**
TNAP
eNPP1
Pit1
Pit2
eNTPD1
ANK
D
Lamin A
Progerin
TNAP
eNTPD1
α-tubulin
Lamin A
Progerin
TNAP/α-tubulin (a.u.)
***
eNTDP1/ α-tubulin (a.u.)
#
E
Extracellular ATP (fmol/μg protein)
#
Intracellular ATP (fmol/μg protein)
*
Mitochondrial ATP synthesis (nmolATP/min/million cell)
#
COX/CS
*
Extracellular PPi (fmol/μg protein)
#
Lamin A
Progerin

FIGURE 5

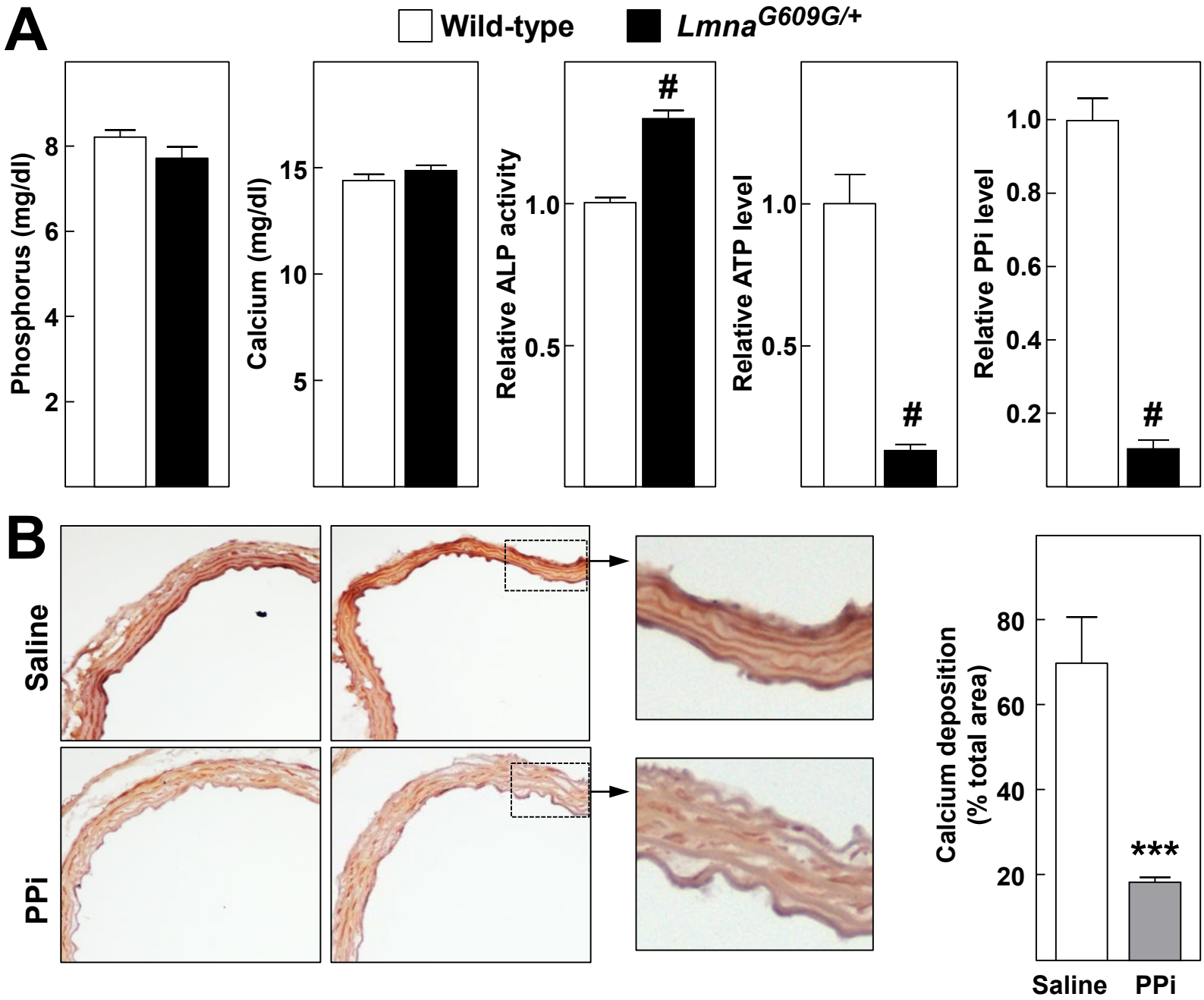
A
Wild-type
Lmna G609G/+
Phosphorus (mg/dl)
8
6
4
2
Calcium (mg/dl)
15
10
5
Relative ALP activity
1.0
0.5
#
Relative ATP level
1.0
0.5
#
Relative PPi level
1.0
0.8
0.6
0.4
0.2
#
B
Saline
PPi
Calcium deposition (% total area)
80
60
40
20
***
Saline
PPi

FIGURE 6

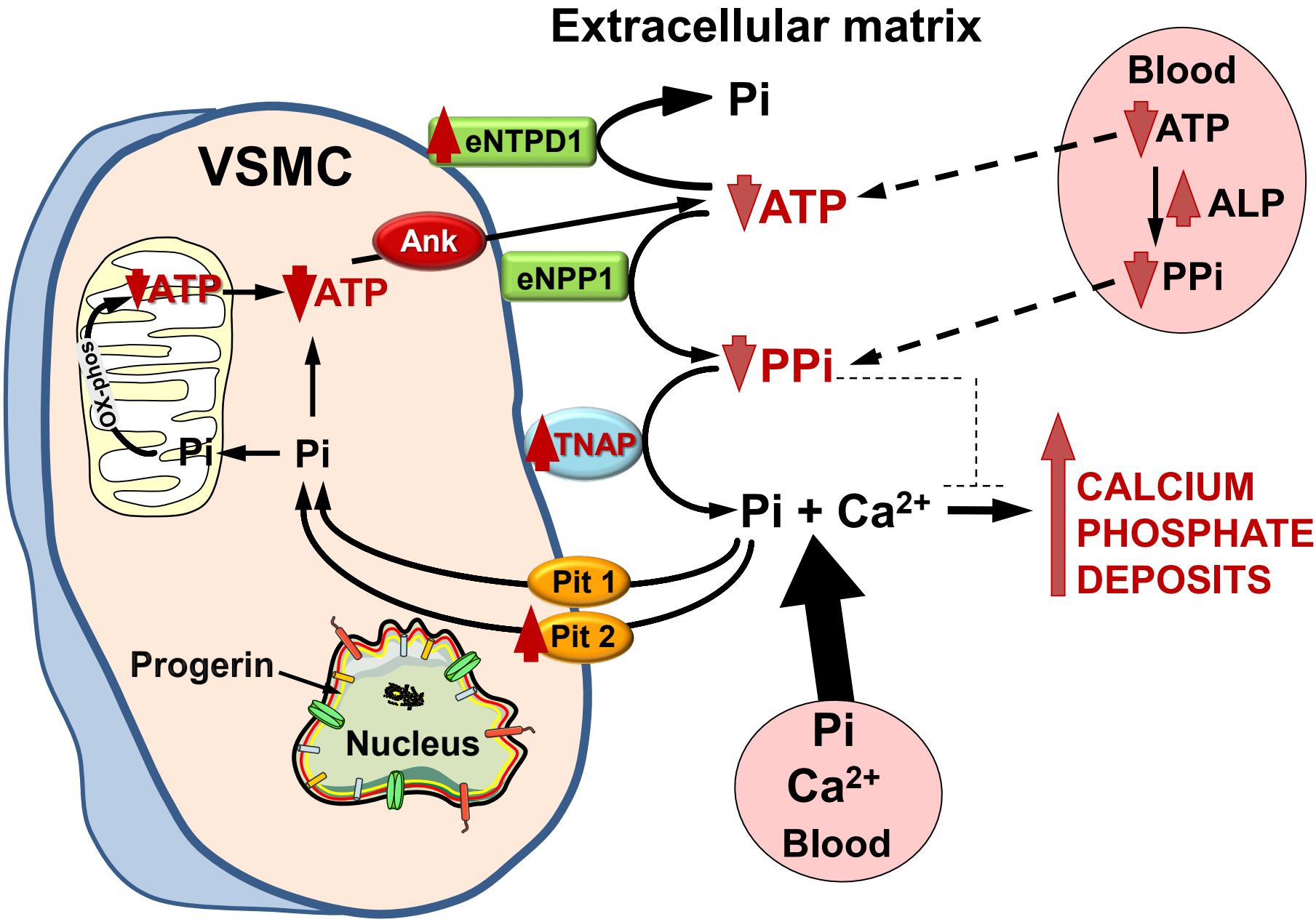
Extracellular matrix
Blood
ATP
ALP
PPi
Pi
VSMC
eNTPD1
ATP
Ank
eNPP1
ATP
ATP
OX-phos
PPi
Pi
Pi
TNAP
Pi + Ca2+
CALCIUM
PHOSPHATE
DEPOSITS
Pit 1
Pit 2
Progerin
Nucleus
Pi
Ca2+
Blood